STUDIA UBB CHEMIA, LVI, 1, 2011

STRUCTURAL INVESTIGATION OF $xFE_2O_3·(70-x)B_2O_3·15ZNO·15CAO$ GLASSES BY INFRARED SPECTROSCOPY AND DFT CALCULATIONS

RĂZVAN ŞTEFAN*[a], EMIL VINȚELER*[b], ALEXANDRU MARCU[b], GEORGETA TARALUNGA[a], SILVANA POPESCU[a], IOAN BRATU[c]

ABSTRACT. The vitreous system $xFe_2O_3·(70-x)B_2O_3·15ZnO·15CaO$ with $0 \leq x \leq 25$ mol% was prepared using the rapid melt quenching method. The effect of Fe_2O_3 on the borate glass structure was investigated by IR spectroscopy and illustrated by Density Functional Theory (DFT) method. The boron atoms are situated in trigonal [BO_3] and tetragonal [BO_4] groups and their ratio depends on Fe_2O_3 content. Two structural models were built, using DFT method, in agreement with IR experimental data, one for base glass $70B_2O_3·15ZnO·15CaO$ (x = 0 mol%) and another for the highest iron content in sample $25Fe_2O_3·45B_2O_3·15ZnO·15CaO$ (x = 25 mol%). Calculations with DFT method show that the addition of iron determines the breaking of B-O bonds in borate network and increases the number of [BO_3] groups.

Keywords: *glass, chemical synthesis, infrared spectroscopy*

INTRODUCTION

Boron glass network has been investigated and the main structural units highlighted by different techniques, one of the most important being the infrared spectroscopy [1]. The borate glass network is built from trigonal [BO_3] units, where every boron atom is situated at the centre of a triangle of oxygen atoms, and boroxol rings $(B_3O_3Ø_3)^0$, which are six-membered planar and regular B_3O_3 rings, connected by three bridging oxygens Ø atoms [1,2].

The addition of oxides (CaO, ZnO or Fe_2O_3) in the borate glass network determines the formation of new structural units such as pentaborate $(B_5O_6Ø_4)^-$, diborate $(B_4O_5Ø_4)^{2-}$, triborate $(B_3O_4Ø_4)^-$ and ditriborate $(B_3O_5Ø_4)^{2-}$ units. These new structural units, containing four-coordinated boron [BO_4] sites, can be revealed by nuclear magnetic resonance [2].

[a] *University of Agricultural Science and Veterinary Medicine, Biophysics Department, Calea Mănăştur 3-5, RO-400372 Cluj-Napoca, Romania, Tel. +40 264 596 384, Int. 207, Fax +40 264 593 792, rstefan@usamvcluj.ro*

[b] *Babeş-Bolyai University, Faculty of Physics, Str. M. Kogălniceanu 1, RO-400084 Cluj-Napoca, Romania, evinteler@phys.ubbcluj.ro*

[c] *National Institute for R&D of Isotopic and Molecular Technology, P.O. Box 700, RO-400293 Cluj-Napoca, Romania*

One can obtain in the binary (100-x)Fe_2O_3·xB_2O_3 system [3], various crystalline phases such as: $FeBO_3$, $FeBO_3$-Fe_3BO_6, α-Fe_2O_3-Fe_3BO_6, depending on preparation condition and compounds ratio. This item of information, about crystalline phases is rather important as it is used in Density Functional Theory (DFT) simulations.

Fe_2O_3 is not a glass network former and this feature makes relatively difficult to prepare glasses containing a high iron oxide content, but for low concentration it acts like a network modifier [4], when it is introduced within borate glass. The glass-forming region of the ternary Fe_2O_3–Bi_2O_3–B_2O_3 system [5] shows that the glass structure can be obtained, in the binary Fe_2O_3–B_2O_3 system, only for molar content of Fe_2O_3 lower than 5%. The addition of zinc, barium and calcium oxides enlarges the glass formation domain in Fe_2O_3–B_2O_3 system up to 25 mol% Fe_2O_3 [6-8].

In the present work, glasses with the molar composition xFe_2O_3·(70-x)B_2O_3·15ZnO·15CaO, with 0 ≤ x ≤ 25 mol%, were prepared. The structure and the effects of Fe_2O_3 on the glass network were investigated by IR spectroscopy. For x = 0 mol% and 25 mol%, two models were built by using DFT method.

RESULTS AND DISCUSSION

IR Spectra of vitreous xFe_2O_3·(70-x)B_2O_3·15ZnO·15CaO system

Figure 1 shows the FT-IR spectra of the xFe_2O_3·(70-x)B_2O_3·15ZnO·15CaO with 0 ≤ x ≤ 25 mol%. The borate glasses FT-IR spectra within range of 400-1600 cm^{-1} were divided in three main regions [1, 9] associated with: bending of B-O-B linkages in the borate network between 400–790 cm^{-1}; B-O bond stretching in tetrahedral [BO_4] units between 790–1140 cm^{-1} and asymmetric B-O stretching vibration in triangular [BO_3] units in the spectral range 1140–1600 cm^{-1}.

Usually in glass IR spectra appear as overlapping bands belonging to various borate units and this feature makes difficult to detect a separate and clear vibrations by IR analysis.

In the above mentioned spectral range, the shapes of bands (Fig. 1) are dependent on Fe_2O_3 molar content, being more narrow for base glass 70B_2O_3·15ZnO·15CaO, while for high iron concentration broad bands appear in the same spectral range.

Thus the shoulder at 1212 cm^{-1}, attributed to B-O bond vibrations in metaborate chains, increases in relative intensity when comparing with band at 1405 cm^{-1}, attributed to B-O bond vibration in [BO_3] units, with the increase of Fe_2O_3 content [10-13]. This denotes the increase in metaborate chains $(B_3O_5Ø_2)^{3-}$ number.

The decrease in relative intensity of the broad band at ~958 cm^{-1}, when comparing with bands at ~849 cm^{-1} and ~1091 cm^{-1}, indicates the decrease of diborate units number, with the increase of Fe_2O_3. The absorption band at 683 cm^{-1}, attributed to B-O-B linkage bending vibration [10] become higher than the envelope that contain $[BO_4]$ specific vibration, i.e., 790-1140 cm^{-1}, during the replacement of B_2O_3 by Fe_2O_3 in the glass composition [9].

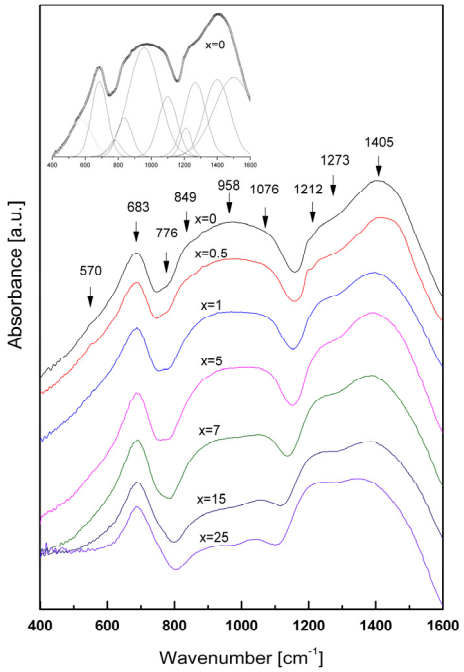

Figure 1. The FT-IR absorption spectra of $xFe_2O_3 \cdot (70\text{-}x)B_2O_3 \cdot 15ZnO \cdot 15CaO$ glasses with $0 \leq x \leq 25$ mol%. In the inset picture the deconvolution bands of FT-IR spectrum for x = 0 mol% is presented

The structural changes associated with the Fe_2O_3 addition have been analyzed on the basis of the ratio $Ar = A_4/A_3$, A_4 and A_3 being calculated as the integral of the absorption signal in the 790-1140 cm^{-1} (A_4) and 1140-1600 cm^{-1} (A_3) spectral ranges [14]. The quantities A_4 and A_3 reflect the relative content of tetrahedral $[BO_4]$ and triangular $[BO_3]$ borate species, respectively. The Ar ratio versus Fe_2O_3 content is given in Figure 2.

For all the investigated glasses, the Ar values are lower than 1, showing the prevalence of $[BO_3]$ units in these glass structures. The presence of $[BO_4]$ units, for x = 0 mol%, in the absence of iron in the glass bulk and the continuous decrease of the Ar ratio demonstrates that the $[BO_4]$ units are replaced by $[BO_3]$ units when the Fe_2O_3 content increases in the glass composition as well as the network modifying role played by Fe cations [6].

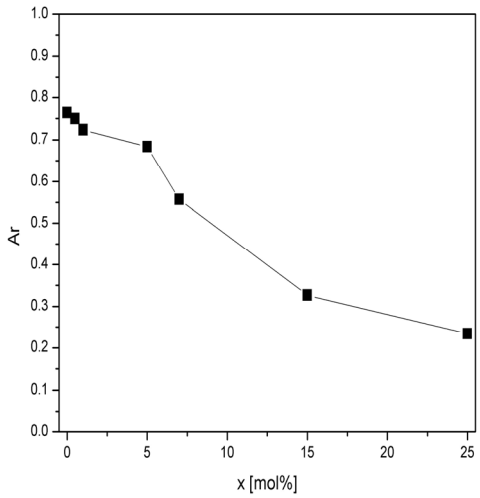

Figure 2. Values of the Ar ratio versus x in $xFe_2O_3 \cdot (70\text{-}x)\ B_2O_3 \cdot 15ZnO \cdot 15CaO$

A more in-depth study of the FT-IR spectra, presenting large bands, characteristic for glasses, needs spectra deconvolution. In the inset of Figure 1 is presented the deconvolution of FT-IR spectrum in the region 400-1600 cm^{-1} for x = 0 mol%. Thus in the region 400-1600 cm^{-1} deconvolution reveals the appearance of 10 bands (for x = 0 mol%) at ~570 cm^{-1}, ~691 cm^{-1}, ~776 cm^{-1}, ~836 cm^{-1}, ~958 cm^{-1}, ~1103 cm^{-1}, ~1212 cm^{-1}, ~1273 cm^{-1}, ~1394 cm^{-1} and ~1503 cm^{-1}, respectively. The deconvoluted spectra for all investigated samples, with characteristic full widths at half maximum (FWHM) and relative areas, are presented in Table 1. The relative area is the component band area divided by the area of the full spectrum in the region 400-1600 cm^{-1}.

The wavenumber bands in spectral range 400-790 cm^{-1}, assigned to borate network bending vibrations, maintain the same spectral position within the investigated compositional range.

The band at ~1212 cm^{-1} (Table 1) shifts to 1181 cm^{-1}, attributed to B-O bond vibrations in pyro- $(B_2O_5)^{4-}$ and orthoborates $(BO_3)^3$, indicating the gradual transformation of metaborate chains into pyro- and orthoborates units.

The band at ~1273 cm^{-1}, attributed to B-O bond vibrations in tri- $(B_3O_4Ø_4)^-$, tetra- $(B_8O_{10}Ø_6)^-$ and pentaborate $(B_5O_6Ø_4)^-$ groups [9, 10, 11], shifts to 1297 cm^{-1}, attributed to B-O bond vibrations [11-13] in pyro- and orthoborates, indicating the transformation of previous mentioned groups into pyro- and orthoborates.

The shift to lower wanumber values of the band at around 1103 cm^{-1} (Table 1) attributed to B-O vibration in $[BO_3]$ units, demonstrates the strong influence of Fe_2O_3 on borate network.

Table 1. Deconvolution parameters of the experimental infrared spectra of $xFe_2O_3·(70-x)B_2O_3·15ZnO·15CaO$ glasses (C is the component band centre (cm^{-1}), W is the band full width at half maximum (cm^{-1}) and A is the relative area (%) of the component band).

x=0	C	**570**	**691**	**776**	**836**	**958**	**1103**	**1212**	**1273**	**1394**	**1503**
	W	158	121	97	109	230	133	73	145	194	230
	A	6	9	2	4	24	8	3	12	14	18
x=0.5	C	**570**	**691**	**776**	**836**	**958**	**1103**	**1212**	**1261**	**1406**	**1503**
	W	158	121	85	109	219	145	73	145	170	230
	A	6	9	2	4	23	9	2	11	15	19
x=1	C	**570**	**691**	**776**	**848**	**958**	**1091**	**1212**	**1261**	**1394**	**1503**
	W	158	109	73	97	218	145	84	158	194	230
	A	7	9	1	4	22	9	3	12	13	20
x=5	C	**570**	**691**	**-**	**836**	**958**	**1091**	**1212**	**1261**	**1394**	**1503**
	W	158	109	-	121	218	133	85	170	218	230
	A	5	9	-	5	22	8	3	13	18	17
x=7	C	**570**	**688**	**-**	**843**	**963**	**1087**	**1204**	**1268**	**1344**	**1469**
	W	158	109	-	121	218	133	85	170	218	230
	A	4	10	-	5	19	7	5	12	9	29
x=15	C	**570**	**690**	**-**	**868**	**989**	**1076**	**1189**	**1299**	**1403**	**1500**
	W	136	113	-	110	183	92	112	188	116	133
	A	3	12	-	4	14	4	9	29	10	15
x= 25	C	**570**	**694**	**-**	**889**	**993**	**1066**	**1181**	**1297**	**1410**	**1500**
	W	141	100	-	98	130	88	114	185	121	102
	A	4	10	-	4	8	4	11	34	15	10

The introduced iron ions break the B-O bond in the vitreous structure and the $[BO_3]$ number increase as well as the nonbridging oxygen atoms O . The more disordered glass structure is illustrated by broadening of the IR absorption lines (Fig. 1) in spectral range 1140-1600 cm^{-1}.

Density Functional Theory Calculations

The spectroscopic results reveal a complex network of iron borate glasses with zinc and calcium formed from di- $(B_4O_5Ø_4)^{2-}$, meta- chain $(B_3O_5Ø_2)^{3-}$, pyro- $(B_2O_5)^{4-}$ and orthoborate $(BO_3)^{3-}$ groups.

For the construction of the models the crystallographic data were utilized for iron borate crystals: vonsenite Fe_3BO_5, Fe_3BO_6 isostructural with nobergite, and $FeBO_3$, isostructural with calcite [16-18]. Thus in the crystal Fe_3BO_6, the iron atoms are six-coordinated by oxygen atoms and are disposed in distorted octahedra and the boron atom is exclusively tetrahedral-coordinated by oxygen atoms. In $FeBO_3$ and Fe_3BO_5 crystals, the boron atom is trigonal-coordinated by oxygen atoms.

Two fully optimized structural models were constructed and are shown in Figures 3a and 3b. The first and the second model simulates the structure of random network of $5B_2O_3 \cdot 1ZnO \cdot 1CaO$ glass (model I in Fig. 3a with 71.43%B_2O_3, 14.285%ZnO and 14.285% CaO) and $2Fe_2O_3 \cdot 3B_2O_3 \cdot 1ZnO \cdot 1CaO$ glass (model II in Fig. 3b with 28.57% Fe_2O_3, 42.86% B_2O_3, 14.285% ZnO and 14.285% CaO), respectively.

The utilized simulation method is able to provide a realistic description of the iron borate glass with zinc and calcium $xFe_2O_3 \cdot (70-x)B_2O_3 \cdot 15ZnO \cdot 15CaO$ for x = 0 mol% and x = 25 mol%.

For each proposed model we performed direct optimization of the geometry with the help of B3LYP/LanL2DZ [19-26] method and using Gaussian 09 program [27].

Frequency analysis followed all optimizations in order to establish the nature of the stationary points found, so that all the reported structures in this study are genuine minima on the potential energy surface, without any imaginary frequencies. For the proposed models we calculated vibrational frequencies with IR absorption intensities using the same method and basis set.

The simulated vibrational frequencies are listed in Table 2 and compared with the values obtained from the deconvolution of experimental spectra for x = 0 and x = 25 mol% (x = moles number of Fe_2O_3 content in glass). A scaling factor of 0.961 was applied to the infrared simulated frequencies.

The bands assignment is in agreement with previous IR studies on borate glasses [9-15].

The two investigated models, describing the random network in the $xFe_2O_3 \cdot (70-x)B_2O_3 \cdot 15ZnO \cdot 15CaO$ glass with x=0 and x=25 mol% are highly possible. The probability to find the simulated structure in vitreous state is higher for a more stable structure with a lower energy per atom. We obtained for, model I without iron, and for model II with iron, the Hartree-Fock energy value per atom E = -50.968 au/atom and E = -65.662 au/atom, respectively.

Table 2. Infrared vibrational properties of $xFe_2O_3 \cdot (70-x)\ B_2O_3 \cdot 15ZnO \cdot 15CaO$ glasses for x = 0 mol% and x = 25 mol% inferred from Gaussian deconvolution of the experimental results and quantum-chemical calculations.

Experimental Frequency [cm^{-1}]		**Theoretical Frequency [cm^{-1}]**		**IR assignment**
x = 0	**x = 25**	**x = 0**	**x = 25**	
570	570	591	568	O-B-O bond bending vibrations
691	694	679	710	B-O-B bond bending vibrations between two [BO_3] units
776	-	777	774	B-O-B bond bending vibrations between [BO_3] and [BO_4] units
836		839		B-O symmetric stretching vibrations in [BO_4] units in borate rings

Experimental Frequency [cm^{-1}]		Theoretical Frequency [cm^{-1}]		IR assignment
x = 0	x = 25	x = 0	x = 25	
	889		872	B-O symmetric stretching vibrations in [BO_4] units from tri-, tetra- and pentaborate groups
958		928 960 992		B-O bond vibrations in diborate groups
	993		933 972	B-O symmetric stretching vibrations in pyro- and orthoborates shifted by Fe cations
	1066		1067 1102	B-O asymmetric stretching vibrations in pyro- and orthoborates shifted by Fe cations
1103		1105 1121		B-O asymmetric stretching vibrations in [BO_4] units in tri-, tetra- and pentaborate groups
1212		1173		B-O bond vibrations in metaborate chains
	1181		1210	B-O bond vibrations in pyro- and orthoborates
1273		1234 1256 1274		B-O asymmetric stretching vibrations in [BO_3] units in tri-, tetra- and pentaborate groups
	1297		1256 1307 1346	B-O asymmetric stretching vibrations in [BO_3] units in pyro- and orthoborates
1394		1383 1399 1428		B-O asymmetric stretching in [BO_3] units in various borate rings
	1410		1413 1428	B-O asymmetric stretching vibrations in [BO_3] units in ortho-borates
1503	1500	1468 1538		$B\text{-}O^-$ bond vibrations

The borate network of model I is build from (Fig. 3a):

i) one diborate unit $(B_4O_5Ø_4)^{2-}$ formed from two trigonal boron atoms B1 and B4 and two tetrahedral boron atoms B2 and B3 linked by a common oxygen atom,

ii) one borate ring unit $(B_4O_4Ø_5)^-$ formed from three trigonal boron atoms B4, B5 and B6 and one tetrahedral boron atom B2,

iii) one metaborate chain unit $(B_3O_5Ø_2)^{3-}$ formed from four trigonal boron atoms B
7, B8, B9 and B10,

iv) one zinc cation (two-coordinated) and one calcium cation (four-coordinated).

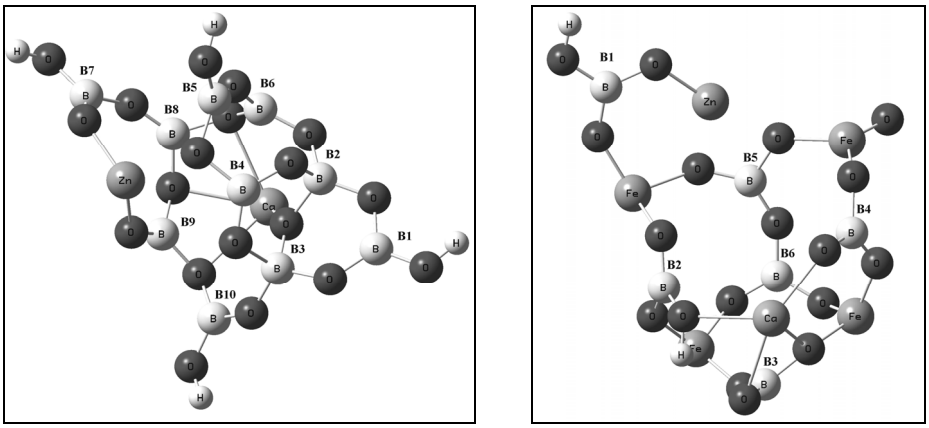

a b

Figure 3. The optimized structures of two possible models obtained by DFT computations: a) $5B_2O_3 \cdot 1ZnO \cdot 1CaO$ glass (model I); b) $2Fe_2O_3 \cdot 3B_2O_3 \cdot 1ZnO \cdot 1CaO$ glass (model II).

The borate network of model II is build from (see Fig. 3b):

i) four orthoborate units $(BO_3)^{3-}$ containing the trigonal boron atoms B1, B2, B3 and B4,

ii) one pyroborate unit $(B_2O_5)^{4-}$ containing the trigonal boron atoms B5 and B6,

iii) four iron cations (three-coordinated), one zinc cation (two-coordinated) and one calcium cation (four-coordinated).

CONCLUSIONS

The addition of iron oxide ($0 \leq x \leq 25$ mol%) to borate $70B_2O_3 \cdot 15ZnO \cdot 15CaO$ glasses, with a high content of B_2O_3, determines important changes in the boron network at intermediate-distance order. By using the infrared spectroscopy the main structural units $[BO_4]$ and $[BO_3]$ of the glass network have been studied and also the gradual conversion of tetrahedral boron units in trigonal ones.

DFT calculations show that the conversion of structural groups as well as creation of new groups at intermediate distance, is due to the insertion of iron cations and the break-up of B-O bonds in borate network as well. DFT calculations are in good agreement with IR experimental spectra of $xFe_2O_3 \cdot (70-x)B_2O_3 \cdot 15ZnO \cdot 15CaO$ vitreous system for x = 0 mol% and x = 25 mol%.

EXPERIMENTAL SECTION

Samples from $xFe_2O_3\cdot(70\text{-}x)B_2O_3\cdot15ZnO\cdot15CaO$ vitreous system with $0 \le x \le 25$ mol% were prepared using pure reagent-grade compounds, i.e., H_3BO_3, Fe_2O_3, ZnO and CaO, in appropriate ratios. The mixtures corresponding to the desired compositions were melted in air, in sintered corundum crucibles, in an electric furnace at 1200ºC, t = 15 min. The melts were quickly cooled to room temperature by pouring onto stainless-steel plates.

The structure of the samples was examined by means of X-ray diffraction using a standard Bruker X D8 Advance diffractometer with a Si monochromator for incident beam in order to obtain only CuKa radiation (λ = 1.5406 Å). The diffractograms have been measured in the range of 2θ = 0-90º. The analysis was made on powdered samples to satisfy the diffraction condition of Bragg. The amorphous nature of the glass under investigation was confirmed by the absence of any sharp peaks in X-ray diffraction patterns.

The Fourier-Transform infrared (FT-IR) absorption spectra were recorded with a JASCO 6100 spectrophotometer, at room temperature, in the range 400-4000 cm^{-1}, with a resolution of 4 cm^{-1}, using the KBr pellet technique.

For each proposed model of $xFe_2O_3\cdot(70\text{-}x)B_2O_3\cdot15ZnO\cdot15CaO$ with x=0 mol% and x=25 mol% we performed direct optimization of the geometry with the help of B3LYP/LanL2DZ method and using Gaussian 09 program [27]. Dangling bonds of outer atoms of the models were saturated with hydrogen atoms. After attaining the equilibrium configuration of the models, we calculated vibrational frequencies with IR absorption intensities using the same method and basis set.

ACKNOWLEDGMENTS

This work was supported by CNCSIS–UEFISCSU, project number 1117 PNII – IDEI code 2528/2008.

REFERENCES

1. Y.D. Yiannopoulos, G.D. Chryssikos, E.I. Kamitsos, *Phys. Chem. Glass*, **2001**, *42*, 164.
2. P.J. Bray, *Inorg. Chim. Acta*, **1999**, *289,* 158.
3. H. Makram, L. Touren, J. Loners, *J. Cryst. Growth*, **1972**, *585,* 13.
4. L. Baia, R. Stefan, J. Popp, S. Simon, W. Kiefer, *J. Non-Cryst. Solids*, **2003**, *324,* 109.
5. H.H. Qiu, T. Ito, H. Sakata, *Mater. Chem. Phys.*, **1999**, *58,* 243.
6. I. Ardelean, P. Pascuta, *Mater. Lett.,* **2004,** *58,* 3499.
7. M. Toderaş, S. Filip, I. Ardelean, *J. Optoelectron. Adv. M.*, **2006**, *8(3),* 1121.

8. S. Hiroshi, *J. Jpn. I. Met.*, **2004**, *68(2),* 152.
9. C.P. Varsamis, E.I. Kamitsos, G.D. Chryssikos, *Solid State Ionics*, **2000**, *136,* 1031.
10. E.I. Kamitsos, M.A. Karakassides, G.D. Chryssikos, *Phys. Chem. Glass*., **1986**, *90,* 4528.
11. S.G. Motke, S.P. Yawale, S.S. Yawale, *Bull. Mater. Sci*., **2002**, *25,* 75.
12. J.F. Ducel, J.J. Videau, M. Couzi, *Phys. Chem. Glasses,* **1993**, *34*, 212.
13. S.P. Yawale, S.V. Pakade, C.S. Adgaonka, *Indian J. Pure Ap. Phy.,* **1995**, *33*, 34.
14. M.S. Gaafar, H.A. Afifi, M.M. Mekaway, *Physica B*, **2009**, *404,* 1668.
15. E.I. Kamitsos, M.A. Karakassides, G.D. Chryssikos, *J. Phys. Chem.*, **1987**, *91,* 1073.
16. J.S. Swinnea, H. Steinfink, *Am. Mineral.*, **1983**, *68,* 827.
17. J.G. White, A. Miller, R.E. Nielsen, *Acta Crystallogr.,* **1965**, *19,* 1060.
18. R. Diehl, *Solid State Commun.*, **1975**, *17(6),* 74.
19. A.D. Becke, *J. Chem. Phys*., **1993**, *98*, 1372.
20. A.D. Becke, *Phys. Rev. A*, **1988**, *38 (6)*, 3098.
21. Chengteh Lee, Weitao Yang and Robert G. Parr, *Phys. Rev. B,* **1988**, *37*, 785.
22. S.H. Vosko, L. Wilk and M. Nusair, *Can. J. Phys.,* **1980**, *58*, 1200.
23. T.H. Dunning Jr., P.J. Hay, In: Modern Theoretical Chemistry, H. F. Schaefer III, Vol. 3 Plenum, New York, **1976**, 1.
24. P.J. Hay and W.R. Wadt, *J. Chem. Phys.*, **1985**, *82*, 270.
25. P.J. Hay and W.R. Wadt, *J. Chem. Phys.*, **1985**, *82*, 299.
26. W.R. Wadt and P.J. Hay, *J. Chem. Phys.*, **1985**, *82,* 284.
27. M.J. Frisch, G.W. Trucks, H.B. Schlegel, G.E. Scuseria, M.A. Robb, J.R. Cheeseman, G. Scalmani, V. Barone, B. Mennucci, G.A. Petersson, H. Nakatsuji, M. Caricato, X. Li, H.P. Hratchian, A.F. Izmaylov, J. Bloino, G. Zheng, J.L. Sonnenberg, M. Hada, M. Ehara, K. Toyota, R. Fukuda, J. Hasegawa, M. Ishida, T. Nakajima, Y. Honda, O. Kitao, H. Nakai, T. Vreven, J. A. Montgomery, Jr., J.E. Peralta, F. Ogliaro, M. Bearpark, J.J. Heyd, E. Brothers, K.N. Kudin, V.N. Staroverov, R. Kobayashi, J. Normand, K. Raghavachari, A. Rendell, J.C. Burant, S.S. Iyengar, J. Tomasi, M. Cossi, N. Rega, J.M. Millam, M. Klene, J.E. Knox, J.B. Cross, V. Bakken, C. Adamo, J. Jaramillo, R. Gomperts, R.E. Stratmann, O. Yazyev, A.J. Austin, R. Cammi, C. Pomelli, J.W. Ochterski, R.L. Martin, K. Morokuma, V.G. Zakrzewski, G.A. Voth, P. Salvador, J.J. Dannenberg, S. Dapprich, A.D. Daniels, Ö. Farkas, J.B. Foresman, J.V. Ortiz, J. Cioslowski, D.J. Fox, Gaussian 09, Revision A.1, Gaussian, Inc., Wallingford CT, **2009**.